

Dynamical phonon laser in coupled active-passive microresonators

Bing He,¹ Liu Yang,² and Min Xiao^{1,3}

¹*Department of Physics, University of Arkansas, Fayetteville, Arkansas 72701, USA*

²*Harbin Engineering University, College of Automation, Harbin, Heilongjiang 150001, China*

³*National Laboratory of Solid State Microstructures and School of Physics, Nanjing University, Nanjing 210093, China*

(Received 7 March 2016; published 13 September 2016)

Effective transition between the population-inverted optical eigenmodes of two coupled microcavities carrying mechanical oscillation realizes a phonon analog of optical two-level lasers. By providing an approach that linearizes the dynamical equations of weak nonlinear systems without relying on their steady states, we study such phonon laser action as a realistic dynamical process, which exhibits time-dependent stimulated phonon field amplification especially when one of the cavities is added with optical gain medium. The approach we present explicitly gives the conditions for the optimum phonon lasing, and thermal noise is found to be capable of facilitating the phonon laser action significantly.

DOI: [10.1103/PhysRevA.94.031802](https://doi.org/10.1103/PhysRevA.94.031802)

Compound structures such as coupled microcavities or waveguides constitute a large number of interesting systems in the optical sciences. An important category that has recently attracted extensive research covers those with alternately distributed active (gain) and passive (loss) components, as they can mimic the parity-time (\mathcal{PT}) symmetric quantum mechanics [1], a generalization of ordinary quantum mechanics. In addition to the theoretical investigations (see, e.g., [2–13]), numerous experiments have demonstrated peculiar features of light transmission in these systems [14–19]. Richer phenomena could manifest if they incorporate other degrees of freedom to form hybrid systems, which have been studied by combining \mathcal{PT} symmetric systems with Kerr nonlinearity [20–25] and mechanical oscillators [26–29].

The device of two coupled microcavities in Fig. 1 can implement phonon laser action [30], as well as in many other systems [31–42]. Here the coupling intensity J of the two microcavities is determined with their adjustable gap. Under a pump drive of the intensity E and frequency ω_L , two eigenmodes or supermodes of different energy levels, as the superpositions of the individual cavity modes, will be built up. If one of the cavities also carries a mechanical oscillation with the frequency ω_m , the cavity supermodes will couple to the associated phonon field in cavity material via radiation pressure. Once there is a population inversion between the cavity supermodes, an amplification of the phonon field will be realized in analogy to an optical laser.

A recent study [26] proposes the enhancement of phonon lasing by adding an optical gain medium into one of the cavities (also see [29] for a continued study in a similar approach). Then the system will have the exact \mathcal{PT} symmetry given the equal gain rate g and loss rate γ of the respective cavities, and this \mathcal{PT} symmetric point was predicted to be capable of achieving the best performance of the phonon laser driven by a resonant pump [26]. A prediction like this was made under the assumption that the phonon laser operates in a steady state, in which the expectation values of the cavity modes \hat{a}_1, \hat{a}_2 and mechanical mode \hat{b} remain unchanged with time.

However, as we will show below, the phonon laser should operate under a blue detuned pump which leads to no steady state. In the presence of optical gain similar systems can be fully dynamical. A well-known example is that, at the

above-mentioned \mathcal{PT} symmetric point $g = \gamma$, the intracavity light fields are totally variable, exhibiting a transition from periodically oscillating to exponentially growing as the cavity coupling J decreases across the exceptional point $J = \gamma$. A slight change of a cavity's size under radiation pressure can hardly make these dynamically evolving fields become time-independent. Properly understanding the concerned phonon laser operation necessitates an approach based on the dynamical picture.

To be more specific, the system's dynamical equations read [43]

$$\dot{\hat{a}}_1 = -(\gamma - ig_m \hat{x})\hat{a}_1 - iJ\hat{a}_2 + Ee^{-i\Delta t} + \sqrt{2\gamma}\hat{\xi}_p, \quad (1)$$

$$\dot{\hat{a}}_2 = g\hat{a}_2 - iJ\hat{a}_1 + \sqrt{2g}\hat{\xi}_a^\dagger, \quad (2)$$

$$\dot{\hat{b}} = -\gamma_m\hat{b} - i\omega_m\hat{b} + ig_m\hat{a}_1^\dagger\hat{a}_1 + \sqrt{2\gamma_m}\hat{\xi}_m \quad (3)$$

in a frame co-moving at the frequency ω_c ($\Delta = \omega_c - \omega_L$) of the two cavities, where $\hat{x} = \hat{b} + \hat{b}^\dagger$ is the dimensionless position operator of the mechanical oscillator damping at the rate γ_m and coupled to the passive mode occupation $\hat{a}_1^\dagger\hat{a}_1$ with a constant $g_m = \omega_c x_0/R$ (x_0 is the mechanical oscillator's zero-point fluctuation and R is the cavity size). Without a classical steady state it will be impossible to linearize the dynamical equations (1)–(3) following the practice in most other works about quantum optomechanics. Moreover, these equations carry the random drive terms of the dissipation (amplification) noise $\hat{\xi}_p$ ($\hat{\xi}_a$) and the thermal noise $\hat{\xi}_m$, which satisfy the relations $\langle \hat{\xi}_i(t)\hat{\xi}_i^\dagger(t') \rangle = \delta(t-t')$ ($i = p, a$) and $\langle \hat{\xi}_m(t)\hat{\xi}_m^\dagger(t') \rangle = (n_{th} + 1)\delta(t-t')$ (n_{th} is the thermal reservoir mean occupation number). The effects of these quantum noises, which are neglected in previous studies but exist in any concerned quantum dynamical process, should be well clarified. In this work we develop an approach to such quantum dynamical processes. The population inversion of the optical supermodes, as the key to the phonon lasing, will be determined in this approach capable of dealing with the quantum noises which are indispensable as shown below.

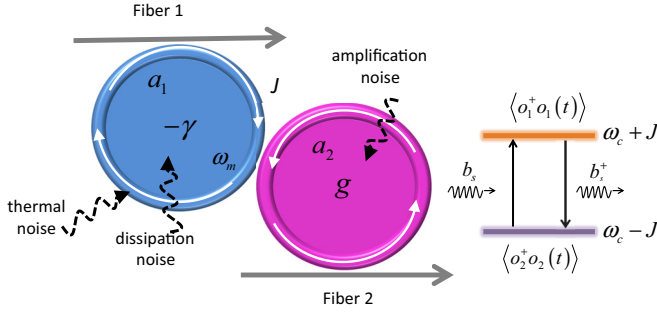


FIG. 1. Setup of coupled microcavities with their coupling rate J adjusted by their gap distance. The first cavity carries a mechanical mode. The pump field from the second optical fiber for amplification does not couple to the first cavity. The stimulated transition of phonons takes place between two supermode states $\hat{\delta}_1^\dagger|0\rangle$ and $\hat{\delta}_2^\dagger|0\rangle$ separated by an energy level difference $2J$, and their occupation numbers $\langle \hat{\delta}_i^\dagger \hat{\delta}_i(t) \rangle$ ($i = 1, 2$) are generally time-dependent in the dynamical operation of the setup.

Our approach makes use of the stochastic Hamiltonian

$$H_{\text{SR}}(t) = i\{\sqrt{2\gamma}[\hat{a}_1^\dagger \hat{\xi}_p(t) - \text{H.c.}] + \sqrt{2g}[\hat{a}_2^\dagger \hat{\xi}_a^\dagger(t) - \text{H.c.}] + \sqrt{2\gamma_m}[\hat{b}^\dagger \hat{\xi}_m(t) - \text{H.c.}]\} \quad (4)$$

in terms of the system-reservoir couplings for the amplification and dissipations in the system (the notation in [25] for the amplification part is adopted). The quantum dynamical equations (1)–(3) can be obtained by the small increments $d\hat{\delta}(t) = U^\dagger(t + dt, t)\hat{\delta}(t)U(t + dt, t) - \hat{\delta}(t)$ of the operators $\hat{\delta} = \hat{a}_1, \hat{a}_2$, and \hat{b} , which are under the evolution $U(t) = \mathcal{T} \exp\{-i \int_0^t d\tau [H_S(\tau) + H_{\text{OM}} + H_{\text{SR}}(\tau)]\}$ of the total Hamiltonian [44]. The Hamiltonians inside the time-ordered exponential include the part

$$H_S(t) = \omega_c \hat{a}_1^\dagger \hat{a}_1 + \omega_c \hat{a}_2^\dagger \hat{a}_2 + \omega_m \hat{b}^\dagger \hat{b} + J(\hat{a}_1 \hat{a}_2^\dagger + \hat{a}_1^\dagger \hat{a}_2) + iE(\hat{a}_1^\dagger e^{-i\omega_L t} - \hat{a}_1 e^{i\omega_L t}) \quad (5)$$

about the cavity coupling plus the external drive, as well as the one $H_{\text{OM}} = -g_m \hat{a}_1^\dagger \hat{a}_1 (\hat{b} + \hat{b}^\dagger)$ about optomechanical interaction.

We apply an interaction picture with respect to the system Hamiltonian $H_S(t)$, whose action $U_0(t) = \mathcal{T} \exp\{-i \int_0^t d\tau H_S(\tau)\}$ evolves the cavity modes as the exact transformation

$$\begin{pmatrix} U_0^\dagger \hat{a}_1 U_0 \\ U_0^\dagger \hat{a}_2 U_0 \end{pmatrix} = \frac{1}{\sqrt{2}} e^{-i\omega_c t} \begin{pmatrix} \frac{\hat{a}_1 + \hat{a}_2}{\sqrt{2}} e^{-iJt} + \frac{\hat{a}_1 - \hat{a}_2}{\sqrt{2}} e^{iJt} \\ \frac{\hat{a}_1 + \hat{a}_2}{\sqrt{2}} e^{-iJt} - \frac{\hat{a}_1 - \hat{a}_2}{\sqrt{2}} e^{iJt} \end{pmatrix} + \sqrt{2} e^{-i\omega_c t} \begin{pmatrix} E_1(t) \\ E_2(t) \end{pmatrix}, \quad (6)$$

where

$$\begin{aligned} E_1(t) &= \frac{iE}{2\sqrt{2}} \left[\frac{1}{\Delta + J} e^{-iJt} + \frac{1}{\Delta - J} e^{iJt} - \frac{2\Delta}{\Delta^2 - J^2} e^{i\Delta t} \right], \\ E_2(t) &= \frac{iE}{\sqrt{2}} \left[\frac{J}{\Delta^2 - J^2} e^{i\Delta t} - \frac{J}{\Delta^2 - J^2} \cos(Jt) - i \frac{\Delta}{\Delta^2 - J^2} \sin(Jt) \right]. \end{aligned} \quad (7)$$

The optical supermodes $\hat{\delta}_{1,2} = (\hat{a}_1 \pm \hat{a}_2)/\sqrt{2}$ with the energy levels $\omega_c \pm J$ naturally appear in Eq. (6). Taking the interaction picture is equivalent to the factorization

$$\begin{aligned} \mathcal{T} e^{-i \int_0^t d\tau [H_S(\tau) + H_{\text{OM}} + H_{\text{SR}}(\tau)]} \\ = U_0(t) \mathcal{T} e^{-i \int_0^t d\tau U_0^\dagger(\tau) [H_{\text{OM}} + H_{\text{SR}}(\tau)] U_0(\tau)} \end{aligned} \quad (8)$$

of the evolution operator $U(t)$ [45], to have the exact form $U_0^\dagger(t)[H_{\text{OM}} + H_{\text{SR}}(t)]U_0(t)$ in one of the time-ordered exponentials above consisting of two parts. One is in a time-dependent quadratic form plus a mechanical displacement term and three system-reservoir coupling terms

$$\begin{aligned} H_1(t) &= -g_m \{ [E_1(t)(\hat{\delta}_1^\dagger e^{iJt} + \hat{\delta}_2^\dagger e^{-iJt}) + \text{H.c.}] \\ &\quad + 2|E_1(t)|^2 (\hat{b} e^{-i\omega_m t} + \hat{b}^\dagger e^{i\omega_m t}) \\ &\quad + i\sqrt{g} \{ [\hat{\delta}_1^\dagger e^{iJt} - \hat{\delta}_2^\dagger e^{-iJt} + 2E_2^*(t)] e^{i\omega_c t} \hat{\xi}_a^\dagger - \text{H.c.} \} \\ &\quad + i\sqrt{\gamma} \{ [\hat{\delta}_1^\dagger e^{iJt} + \hat{\delta}_2^\dagger e^{-iJt} + 2E_1^*(t)] e^{i\omega_c t} \hat{\xi}_p - \text{H.c.} \} \\ &\quad + i\sqrt{2\gamma_m} \{ \hat{b}^\dagger e^{i\omega_m t} \hat{\xi}_m(t) - \text{H.c.} \}, \end{aligned} \quad (9)$$

and the other is the cubic nonlinear one

$$\begin{aligned} H_2(t) &= -\frac{1}{2} g_m (\hat{\delta}_1^\dagger e^{iJt} + \hat{\delta}_2^\dagger e^{-iJt}) (\hat{\delta}_1 e^{-iJt} + \hat{\delta}_2 e^{iJt}) \\ &\quad \times (\hat{b} e^{-i\omega_m t} + \hat{b}^\dagger e^{i\omega_m t}). \end{aligned} \quad (10)$$

The terms containing $\hat{\delta}_1 \hat{\delta}_2^\dagger \hat{b}^\dagger$ or its conjugate in the second Hamiltonian $H_2(t)$ indicate a transition from the blue supermode $\hat{\delta}_1$ to the red supermode $\hat{\delta}_2$ while generating a phonon (see the level scheme in Fig. 1), realizing phonon lasing once the occupation of the blue supermode surpasses that of the red one. The Hamiltonian $H_2(t)$ also gives the resonant transition between the two supermodes at $\omega_m = 2J$, i.e., the coefficient of $\hat{\delta}_1 \hat{\delta}_2^\dagger \hat{b}^\dagger$ becomes unity, corresponding to the gain spectrum line center of the stimulated phonon field [30].

Under the simultaneous action of $H_1(t)$ and $H_2(t)$, the supermode populations

$$\begin{aligned} \langle \hat{\delta}_i^\dagger \hat{\delta}_i(t) \rangle &= \text{Tr}_S [\hat{\delta}_i^\dagger \hat{\delta}_i \rho_S(t)] \\ &= \text{Tr}_S \{ \hat{\delta}_i^\dagger \hat{\delta}_i \text{Tr}_R [U(t) \rho_S(0) \rho_R U^\dagger(t)] \}, \end{aligned} \quad (11)$$

for $i = 1, 2$, are predominantly determined by the former. Here $\rho_S(t)$ and ρ_R are the reduced system state and the total reservoir state, respectively. This can be seen from their following reduction:

$$\begin{aligned} \langle \hat{\delta}_i^\dagger \hat{\delta}_i(t) \rangle &= \text{Tr}_{S,R} \{ \hat{\delta}_i^\dagger \hat{\delta}_i U_0(t) \mathcal{T} e^{-i \int_0^t d\tau (H_1 + H_2)(\tau)} \\ &\quad \times \rho_S(0) \rho_R \mathcal{T} e^{i \int_0^t d\tau (H_1 + H_2)(\tau)} U_0^\dagger(t) \} \\ &\approx \text{Tr}_{S,R} \{ U_1^\dagger(t) U_0^\dagger(t) \hat{\delta}_i^\dagger \\ &\quad \times \hat{\delta}_i U_0(t) U_1(t) U_2(t) \rho_S(0) \rho_R U_2^\dagger(t) \} \\ &= \text{Tr}_{S,R} \{ U_1^\dagger(t) U_0^\dagger(t) \hat{\delta}_i^\dagger \hat{\delta}_i U_0(t) U_1(t) \rho_S(0) \rho_R \}, \end{aligned} \quad (12)$$

where $U_l(t) = \mathcal{T} e^{-i \int_0^t d\tau H_l(\tau)}$ for $l = 1, 2$. In Eq. (12), the relation $U_2(t) \rho_S(0) U_2^\dagger(t) = \rho_S(0)$ for the system's initial state $\rho_S(0)$, the product of a cavity vacuum state $|0\rangle_c$ and a mechanical thermal state, is due to the fact $H_2(t)|0\rangle_c = 0$. The approximate equality in Eq. (12) comes from factorizing the actions of the noncommutative Hamiltonians $H_1(t)$ and

$H_2(t)$ as

$$\begin{aligned} \mathcal{T}e^{-i\int_0^t d\tau(H_1+H_2)(\tau)} &= \mathcal{T}e^{-i\int_0^t d\tau U_2(t,\tau)H_1(\tau)U_2^\dagger(t,\tau)}U_2(t) \\ &\approx U_1(t)U_2(t). \end{aligned} \quad (13)$$

For the experimentally realizable optomechanical systems of weak coupling, the corrections to the system operators by the unitary operation $U_2(t,\tau) = \mathcal{T}e^{-i\int_\tau^t dt' H_2(t')}$ are in the higher orders of the coefficient $g_m/\omega_m \ll 1$ [46], so that they can be well neglected to use the original form of $H_1(\tau)$ in the time-ordered exponential on the right side of the above equation. This only approximation we use in the calculations of the optical supermode populations is independent of the drive intensity E .

While the unitary operation $U_0(t)$ only displaces the supermode operators in Eq. (12), the action $U_1(t)$ of the Hamiltonian $H_1(t)$ leads to the following dynamical equations [44]:

$$\begin{aligned} \dot{\hat{\delta}}_1 &= 1/2(g - \gamma)\hat{\delta}_1 + 1/2(g + \gamma)e^{2iJt}\hat{\delta}_2 \\ &\quad + ig_m E_1(t)e^{iJt}(\hat{b}e^{-i\omega_m t} + \hat{b}^\dagger e^{i\omega_m t}) \\ &\quad + [\gamma E_1(t) - gE_2(t)]e^{iJt} + \hat{n}_1(t), \\ \dot{\hat{\delta}}_2 &= 1/2(g + \gamma)e^{-2iJt}\hat{\delta}_1 + 1/2(g - \gamma)\hat{\delta}_2 \\ &\quad + ig_m E_1(t)e^{-iJt}(\hat{b}e^{-i\omega_m t} + \hat{b}^\dagger e^{i\omega_m t}) \\ &\quad + [\gamma E_1(t) + gE_2(t)]e^{-iJt} + \hat{n}_2(t), \\ \dot{\hat{b}} &= -\gamma_m \hat{b} + ig_m E_1^*(t)e^{i\omega_m t}(\hat{\delta}_1 e^{-iJt} + \hat{\delta}_2 e^{iJt}) \\ &\quad + ig_m E_1(t)e^{i\omega_m t}(\hat{\delta}_1^\dagger e^{iJt} + \hat{\delta}_2^\dagger e^{-iJt}) \\ &\quad + 2ig_m |E_1(t)|^2 e^{i\omega_m t} + \hat{n}_3(t) \end{aligned} \quad (14)$$

for the system operators, where

$$\begin{aligned} \hat{n}_1(t) &= \sqrt{g}e^{iJt}e^{i\omega_c t}\hat{\xi}_a^\dagger(t) + \sqrt{\gamma}e^{iJt}e^{i\omega_c t}\hat{\xi}_p(t), \\ \hat{n}_2(t) &= \sqrt{g}e^{-iJt}e^{i\omega_c t}\hat{\xi}_a^\dagger(t) - \sqrt{\gamma}e^{-iJt}e^{i\omega_c t}\hat{\xi}_p(t), \\ \hat{n}_3(t) &= \sqrt{2\gamma_m}e^{i\omega_m t}\hat{\xi}_m(t). \end{aligned} \quad (15)$$

The noise drive terms in Eq. (15) must be included in these equations. For example, in the trivial situation of turning off the pump drive ($E = 0$), the damping of the mechanical mode would result in its ‘‘cooling’’ to the ground state, i.e., $\langle \hat{b}^\dagger \hat{b}(t) \rangle \rightarrow 0$ as $t \rightarrow \infty$, were there no thermal noise term $\hat{n}_3(t)$ in the last equation of (14). The invariant occupation number $\langle \hat{b}^\dagger \hat{b} \rangle$ under such thermal equilibrium is preserved with the complete form $\hat{b}(t) = e^{-\gamma_m t} \hat{b} + \sqrt{2\gamma_m} \int_0^t d\tau e^{-\gamma_m(t-\tau)} e^{i\omega_m \tau} \hat{\xi}_m(\tau)$ of the evolved mechanical mode. The evolved supermodes $\hat{\delta}_1(t), \hat{\delta}_2(t)$, on the same footing with $\hat{b}(t)$ in Eq. (14), should include the contributions from the quantum noises as well.

The next question is how to evolve the supermodes so that a good population inversion $\Delta N(t) = \langle \hat{\delta}_1^\dagger \hat{\delta}_1(t) \rangle - \langle \hat{\delta}_2^\dagger \hat{\delta}_2(t) \rangle$ can be achieved. One advantage of our approach is that the conditions for realizing the optimal population inversion can be straightforwardly read from Eq. (14), which is an inhomogeneous system of differential equations with the coherent and noise drive terms. The coefficients of $\hat{\delta}_i$ or $\hat{\delta}_i^\dagger$ on the right side of the last equation, for example, are generally the sums of complex exponential functions of t considering the form of $E_1(t)$. These coefficients reflect the

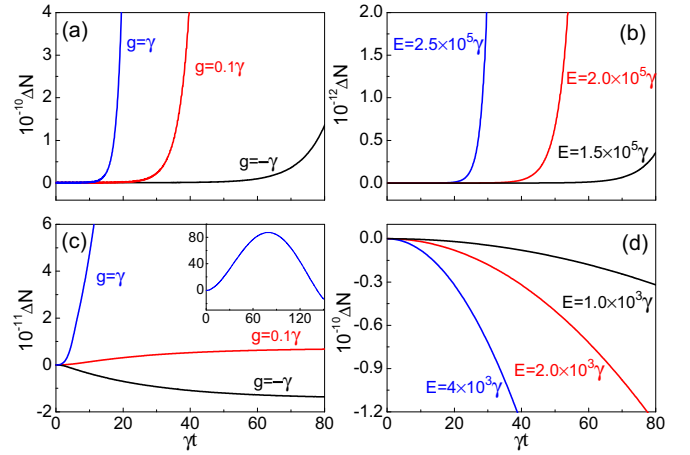


FIG. 2. Population inversion evolutions in a setup with the system parameters $\omega_m = 22.8\gamma$, $g_m = 5 \times 10^{-5}\gamma$, and $\gamma_m = 0.037\gamma$, which are converted from those of the experiment in [30]. The setup operates under the optimal transition condition $\omega_m = 2J$ and in an environment of $T = 273$ K ($n_{th} = 2.4 \times 10^5$). The choice of the other parameters: (a) $E = 2.5 \times 10^5\gamma$, $\Delta = -3J$; (b) $g = 0.5\gamma$, $\Delta = -3J$; (c) $E = 10^7\gamma$, $\Delta = 0$; (d) $g = 0.5\gamma$, $\Delta = J$. The inserted plot in (c) shows the long-term behavior for the curve of $g = \gamma$.

intensities of the beam splitter (BS) type coupling in the form $f(t)\hat{\delta}_i\hat{b}^\dagger + \text{H.c.}$ or the squeezing (SQ) type coupling in the form $g(t)\hat{\delta}_i^\dagger\hat{b}^\dagger + \text{H.c.}$, where the exact functions $f(t), g(t)$ can be found from Eq. (9). These couplings can be enhanced if a complex exponential function of t in $f(t)$ or $g(t)$ becomes unity. A significant population inversion will be realized if an SQ coupling between the blue supermode $\hat{\delta}_1$ and the mechanical mode \hat{b} can be strengthened. Such enhancement will be possible by setting the pump to blue sideband with its detuning Δ equal to $-\omega_m - J = -3J$ [considering the optimal transition condition $\omega_m = 2J$ from Eq. (10)], reducing the factor $e^{i(\Delta + \omega_m + J)t}$ before $\hat{\delta}_1^\dagger$ in the last equation of (14) to a unity.

To illustrate the general theory, we plot the population inversions in terms of the dimensionless parameters in Fig. 2. These inversions are numerically calculated with Eq. (14). Figures 2(a) and 2(b) show that, under the above-mentioned two optimal conditions, the inversions grow with time due to the SQ process. Increased gain rate g and drive intensity E serve as the additional factors to make them go up monotonically farther. The inversion in a passive setup ($g = -\gamma$) can increase with time, in addition to reaching the steady states (not shown here) under lower drive intensity E for this passive setup (in the absence of considerably high optical gain, steady states may exist under the condition $g_m|\alpha_i| \ll \gamma$ for a blue detuned drive, where α_i are the average cavity field amplitudes proportional to the drive intensity E ; see, e.g., a proposed setup in [47]). The enhanced SQ process heats up the cavity material with increased thermal occupation $\langle \hat{b}^\dagger \hat{b}(t) \rangle$ different from the quantity $|\langle \hat{b}(t) \rangle|^2$, and the very strong light fields after a long period will make the system go beyond the current model of linear amplification and dissipation in accordance with the specific material properties.

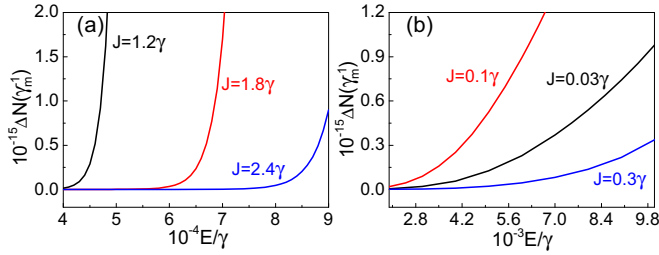


FIG. 3. Relations between the realized population inversion at $t = \gamma_m^{-1}$ and the drive intensity, under the conditions $\omega_m = 2J$ and $\Delta = -\omega_m - J$. Here we set $g = 0.5\gamma$. The regimes of $J > \gamma$ and $J < \gamma$ are illustrated in (a) and (b), respectively. The other fixed system parameters are the same as those in Fig. 2. At a fixed E , the inversion increases with the lowered J from 0.3γ to 0.1γ , but drops as J is decreased further to 0.03γ .

As a comparison we also present two other examples. The first one in Fig. 2(c) is to drive the passive cavity resonantly at $\Delta = 0$, having $E_1(t) = iE/(2\sqrt{2}J)(e^{-iJt} - e^{iJt})$. The term with the factor e^{-iJt} in the $E_1(t)$ provides enhanced SQ coupling between $\hat{\delta}_2$ and \hat{b} , while the one with e^{iJt} enhances the BS coupling between $\hat{\delta}_1$ and \hat{b} , showing that the SQ effect will dominate in the end. The other example in Fig. 2(d) has $\Delta = J$, which happens to be one of the resonant points of the coupled system so that $E_1(t) = iE/(4\sqrt{2}J)[e^{-iJt} - 2(1 + iJt)e^{iJt}]$. In this special situation, the extra linearly increasing factor overshadows the effects of the phase factors ($e^{\pm iJt}$) and nonetheless enhances the SQ coupling between $\hat{\delta}_2$ and \hat{b} , to give negative population inversions.

The influence of the cavity coupling intensity on supermode population inversion is illustrated in Fig. 3, showing the relations between the inversion (at the mechanical oscillation lifetime γ_m^{-1}) and the drive intensity for different J . To keep the optimal conditions in Fig. 2(a), the mechanical frequency ω_m is also assumed to be adjustable in the illustrations. One sees that, given a fixed drive intensity E , a lowered coupling J actually increases the population inversion until it becomes small enough to have the two cavities almost decoupled. This is totally contrasting to the prediction of no phonon lasing in the regime $J < (g + \gamma)/2$ by a previous study [26]. That conclusion is based on the diagonalized form $(\omega_+ + i\gamma_+) \hat{q}_2^\dagger \hat{q}_2 + (\omega_- + i\gamma_-) \hat{q}_1^\dagger \hat{q}_1$ of the non-Hermitian Hamiltonian $(\omega_c - i\gamma) \hat{a}_1^\dagger \hat{a}_1 + (\omega_c + i\gamma) \hat{a}_2^\dagger \hat{a}_2 + J(\hat{a}_1^\dagger \hat{a}_2 + \hat{a}_2^\dagger \hat{a}_1)$ widely used in the study of \mathcal{PT} symmetric optical systems, suggesting that phonons induce a transition between the modes \hat{q}_1, \hat{q}_2 with their gap $\omega_+ - \omega_-$ disappearing when $J < (g + \gamma)/2$. In fact, these generally nonorthogonal modes (see more detailed discussion in [15]) coincide with the supermodes $\hat{\delta}_1, \hat{\delta}_2$ only in a special situation of $g = -\gamma$ [46]. Similarly to the transitions between atomic levels, the action of the Hermitian Hamiltonian $H_2(t)$ can only cause an effective transition between two orthogonal states such as $\hat{\delta}_1^\dagger|0\rangle$ and $\hat{\delta}_2^\dagger|0\rangle$, and the transition between the nonorthogonal states $\hat{q}_1^\dagger|0\rangle$ and $\hat{q}_2^\dagger|0\rangle$ with $\langle 0|\hat{q}_1\hat{q}_2^\dagger|0\rangle \neq 0$ is forbidden for arbitrary system parameters.

A unique property of the optical medium is that the quantum noises, which must be considered as mentioned before, can significantly affect the supermode populations. We illustrate

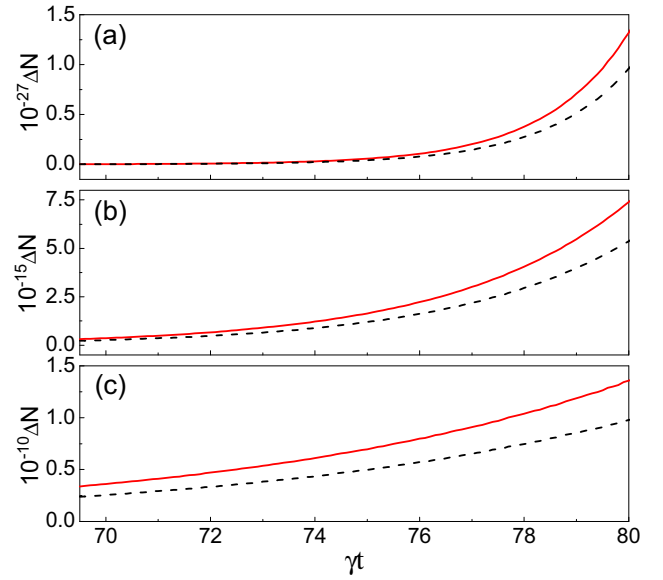


FIG. 4. Thermal noise contribution to the supermode population inversion. The solid curves in (a), (b), and (c) are the portions of those in Fig. 2(a), with $g = \gamma, 0.1\gamma$, and $-\gamma$, respectively. The dashed curves represent the contributions from the thermal noise drive \hat{n}_3 in Eq. (15).

this important fact in Fig. 4 showing the proportions of the thermal noise contribution in the results of Fig. 2(a). The detailed calculation of the noise contributions can be found in [46]. It is seen from the comparisons in Fig. 4 that, under the enhanced SQ coupling due to the properly chosen system parameters, the thermal noise acting as a random drive can predominantly contribute to the population inversions. The contribution is proportional to the thermal occupation number n_{th} , a parameter of the environment. This observation constitutes an interesting feature of the quantum noises which have been seldom discussed for coupled gain-loss systems [4,7,25,48].

With the above understandings, one will find how well the phonon laser can operate. In analogy to an optical laser [49], the phonon laser dynamical equations similar to those in [30] are independently found as

$$\begin{aligned} \dot{b}_s &= (-\gamma_m - i\omega_m)b_s - (1/2)ig_m p, \\ \dot{p} &= (1/2)ig_m \Delta N(t)b_s + [1/2(g - \gamma) - 2iJ]p, \end{aligned} \quad (16)$$

where $b_s = \langle \hat{b}_s \rangle$ [the subscript “s” indicates the stimulated phonon mode to be distinguished from the thermal phonon mode in Eq. (14)] and $p = \langle \hat{\delta}_2^\dagger \hat{\delta}_1 \rangle$. Corresponding to the semiclassical treatment of atomic level transitions, by which the atomic levels are described quantum mechanically while the radiations are regarded as classical, we approximate the phonon laser mode in Eq. (16) as a mean field but insert the inversion $\Delta N(t)$ determined in a completely quantum way from Eq. (14) into the same equations. The amplification rates of the stimulated phonon field numerically found with the above equations are illustrated in Fig. 5. The threshold drive intensity E_{th} for realizing phonon field amplification becomes lower with increased gain rate g , which is upper bounded in reality due to gain saturation. Under the optimal transition

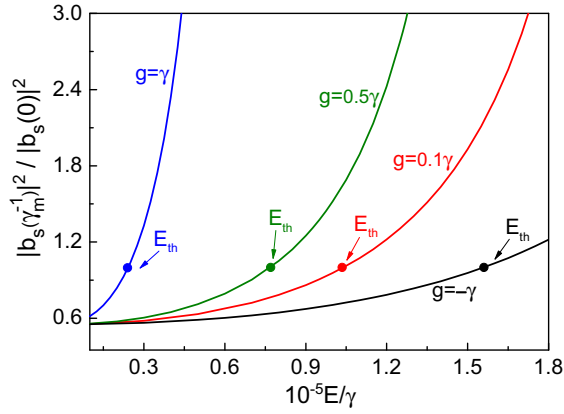


FIG. 5. Amplification of the stimulated phonon field intensity in terms of the ratio between their values at $t = \gamma_m^{-1}$ and $t = 0$. The system parameters are the same as those in Fig. 2(a).

and optimal population inversion condition as in Figs. 2(a) and 2(b), adding optical gain medium into one cavity can enhance the phonon lasing further.

In summary, we have presented a dynamical approach to the phonon laser model of coupled active-passive resonators, which only uses a single approximation in Eq. (13) to make the calculations of the optical supermode populations highly accurate to the system with $g_m \ll \omega_m$. Compared with a previous study based on the assumed steady states for such system [26], we find three fundamental differences: (1) the

phonon laser should operate under a blue-detuned pump rather than the resonant and red-detuned ones considered in [26]—under blue-detuned drives the phonon laser performance simply better with increased optical gain instead of reaching the optimum at the balanced gain and loss; (2) the phonon laser can operate even better in the \mathcal{PT} symmetry broken regime [$J < (g + \gamma)/2$] in contrast to its nonexistence predicted in [26]; (3) under the conditions to realize the optimum lasing, quantum noises can significantly contribute to the supermode population inversion for magnifying the stimulated phonon field. These features surely exist in the presence of the realistic gain saturation, though we use a model of fixed gain rate to illustrate them more clearly. According to our dynamical picture, the optimum phonon lasing in any similar setup (beyond those carrying optical gain) should be reached by choosing a proper pump detuning Δ and a suitable cavity coupling J , and the added optical gain highlighted in [26] will not help the laser action unless the pump detuning is within the appropriate range. For the experimentally realizable optomechanical systems ($g_m/\gamma \ll 1$), the approach can be applied to quantum dynamical processes in the blue-detuned regime, where the previously available approach of classical dynamics (see Sec. VIII in [50]) is unable to deal with the problems involving quantum noises. This approach of linearizing the dynamical equations of weak nonlinear systems without relying on their steady states may be applied to solve other dynamical problems.

M.X. acknowledges partial funding support from NBRPC (Grant No. 2012CB921804) and NSFC (Grant No. 61435007).

- [1] C. M. Bender and S. Boettcher, *Phys. Rev. Lett.* **80**, 5243 (1998).
- [2] R. El-Ganainy, K. G. Makris, D. N. Christodoulides, and Z. H. Musslimani, *Opt. Lett.* **32**, 2632 (2007).
- [3] S. Klaiman, U. Günther, and N. Moiseyev, *Phys. Rev. Lett.* **101**, 080402 (2008).
- [4] H. Schomerus, *Phys. Rev. Lett.* **104**, 233601 (2010).
- [5] Y. D. Chong, L. Ge, and A. D. Stone, *Phys. Rev. Lett.* **106**, 093902 (2011).
- [6] Z. Lin, H. Ramezani, T. Eichelkraut, T. Kottos, H. Cao, and D. N. Christodoulides, *Phys. Rev. Lett.* **106**, 213901 (2011).
- [7] G. S. Agarwal and K. Qu, *Phys. Rev. A* **85**, 031802(R) (2012).
- [8] C. M. Bender, M. Gianfreda, S. K. Özdemir, B. Peng, and L. Yang, *Phys. Rev. A* **88**, 062111 (2013).
- [9] X. Luo, J. Huang, H. Zhong, X. Qin, Q. Xie, Yu. S. Kivshar, and C. Lee, *Phys. Rev. Lett.* **110**, 243902 (2013).
- [10] R. El-Ganainy, M. Khajavikhan, and L. Ge, *Phys. Rev. A* **90**, 013802 (2014).
- [11] M. H. Teimourpour, R. El-Ganainy, A. Eisfeld, A. Szameit, and D. N. Christodoulides, *Phys. Rev. A* **90**, 053817 (2014).
- [12] S. Longhi, *Opt. Lett.* **40**, 5694 (2015).
- [13] B. He, L. Yang, Z. Zhang, and M. Xiao, *Phys. Rev. A* **91**, 033830 (2015).
- [14] A. Guo, G. J. Salamo, D. Duchesne, R. Morandotti, M. Volatier-Ravat, V. Aimez, G. A. Siviloglou, and D. N. Christodoulides, *Phys. Rev. Lett.* **103**, 093902 (2009).
- [15] C. E. Rüter, K. G. Makris, R. El-Ganainy, D. N. Christodoulides, M. Segev, and D. Kip, *Nat. Phys.* **6**, 192 (2010).
- [16] A. Regensburger, C. Bersch, M. A. Miri, G. Onishchukov, D. N. Christodoulides, and U. Peschel, *Nature (London)* **488**, 167 (2012).
- [17] T. Eichelkraut, R. Heilmann, S. Weimann, S. Stützer, F. Dreisow, D. N. Christodoulides, S. Nolte, and A. Szameit, *Nat. Commun.* **4**, 2533 (2013).
- [18] L. Chang, X. Jiang, S. Hua, C. Yang, J. Wen, L. Jiang, G. Li, G. Wang, and M. Xiao, *Nat. Photonics* **8**, 524 (2014).
- [19] B. Peng, S. K. Özdemir, F. Lei, F. Monifi, M. Gianfreda, G. L. Long, S. Fan, F. Nori, C. M. Bender, and L. Yang, *Nat. Phys.* **10**, 394 (2014).
- [20] H. Ramezani, T. Kottos, R. El-Ganainy, and D. N. Christodoulides, *Phys. Rev. A* **82**, 043803 (2010).
- [21] A. A. Sukhorukov, Z. Y. Xu, and Yu. S. Kivshar, *Phys. Rev. A* **82**, 043818 (2010).
- [22] S. V. Dmitriev, A. A. Sukhorukov, and Yu. S. Kivshar, *Opt. Lett.* **35**, 2976 (2010).
- [23] S. V. Suchkov, B. A. Malomed, S. V. Dmitriev, and Yu. S. Kivshar, *Phys. Rev. E* **84**, 046609 (2011).
- [24] D. A. Zezyulin and V. V. Konotop, *Phys. Rev. Lett.* **108**, 213906 (2012).
- [25] B. He, S.-B. Yan, J. Wang, and M. Xiao, *Phys. Rev. A* **91**, 053832 (2015).
- [26] H. Jing, S. K. Özdemir, X.-Y. Lü, J. Zhang, L. Yang, and F. Nori, *Phys. Rev. Lett.* **113**, 053604 (2014).
- [27] X.-W. Xu, Y.-X. Liu, C.-P. Sun, and Y. Li, *Phys. Rev. A* **92**, 013852 (2015).

- [28] X.-Y. Lü, H. Jing, J.-Y. Ma, and Y. Wu, *Phys. Rev. Lett.* **114**, 253601 (2015).
- [29] D. W. Schönleber, A. Eisfeld, and R. El-Ganainy, *New J. Phys.* **18**, 045014 (2016).
- [30] I. S. Grudinin, H. Lee, O. Painter, and K. J. Vahala, *Phys. Rev. Lett.* **104**, 083901 (2010).
- [31] T. Carmon, H. Rokhsari, L. Yang, T. J. Kippenberg, and K. J. Vahala, *Phys. Rev. Lett.* **94**, 223902 (2005).
- [32] M. Tomes and T. Carmon, *Phys. Rev. Lett.* **102**, 113601 (2009).
- [33] K. Vahala, M. Herrmann, S. Knünz, V. Batteiger, G. Saathoff, T. W. Hänsch, and Th. Udem, *Nat. Phys.* **5**, 682 (2009).
- [34] I. S. Grudinin, A. B. Matsko, and L. Maleki, *Phys. Rev. Lett.* **102**, 043902 (2009).
- [35] G. Bahl, J. Zehnpfennig, M. Tomes, and T. Carmon, *Nat. Commun.* **2**, 403 (2011).
- [36] G. Anetsberger, E. M. Weig, J. P. Kotthaus, and T. J. Kippenberg, *C. R. Phys.* **12**, 800 (2011).
- [37] S. Zaitsev, A. K. Pandey, O. Shtempluck, and E. Buks, *Phys. Rev. E* **84**, 046605 (2011).
- [38] J. B. Khurgin, M. W. Pruessner, T. H. Stievater, and W. S. Rabinovich, *Phys. Rev. Lett.* **108**, 223904 (2012).
- [39] I. Mahboob, K. Nishiguchi, A. Fujiwara, and H. Yamaguchi, *Phys. Rev. Lett.* **110**, 127202 (2013).
- [40] U. Kemiktarak, M. Durand, M. Metcalfe, and J. Lawall, *Phys. Rev. Lett.* **113**, 030802 (2014).
- [41] O. Suchoi, K. Shlomi, L. Ella, and E. Buks, *Phys. Rev. A* **91**, 043829 (2015).
- [42] J. D. Cohen, S. M. Meenehan, G. S. MacCabe, S. Gröblacher, A. H. Safavi-Naeini, F. Marsili, M. D. Shaw, and O. Painter, *Nature (London)* **520**, 522 (2015).
- [43] The notation $\hbar = 1$ is used.
- [44] C. W. Gardiner and P. Zoller, *Quantum Noise* (Springer-Verlag, Berlin, 2000).
- [45] G. D. Mahan, *Many-Particle Physics* (Kluwer Academic/Plenum Publishers, New York, 2000), Eq. (2.189).
- [46] See Supplemental Material at <http://link.aps.org/supplemental/10.1103/PhysRevA.94.031802> for detailed derivation and/or discussion.
- [47] N. Lörch and K. Hammerer, *Phys. Rev. A* **91**, 061803(R) (2015).
- [48] K. V. Keesidis, T. J. Milburn, J. Huber, K. G. Makris, S. Rotter, and P. Rabl, *New J. Phys.* **18**, 095003 (2016).
- [49] M. O. Scully and M. S. Zubairy, *Quantum Optics* (Cambridge University Press, Cambridge, UK, 1997).
- [50] M. Aspelmeyer, T. J. Kippenberg, and F. Marquardt, *Rev. Mod. Phys.* **86**, 1391 (2014).